

# Probing the octupole deformation of $^{238}\text{U}$ in high-energy nuclear collisions

Chunjian Zhang,<sup>1,2,3,\*</sup> Jianguo Jia,<sup>3,4,†</sup> Jinhui Chen,<sup>1,2,‡</sup> Chun Shen,<sup>5,6,§</sup> and Lumeng Liu<sup>7,¶</sup>

<sup>1</sup>Key Laboratory of Nuclear Physics and Ion-beam Application (MOE),  
and Institute of Modern Physics, Fudan University, Shanghai 200433, China

<sup>2</sup>Shanghai Research Center for Theoretical Nuclear Physics, NSFC and Fudan University, Shanghai 200438, China

<sup>3</sup>Department of Chemistry, Stony Brook University, Stony Brook, NY 11794, USA

<sup>4</sup>Physics Department, Brookhaven National Laboratory, Upton, NY 11976, USA

<sup>5</sup>Department of Physics and Astronomy, Wayne State University, Detroit, Michigan 48201, USA

<sup>6</sup>RIKEN BNL Research Center, Brookhaven National Laboratory, Upton, New York 11973, USA

<sup>7</sup>Physics Department and Center for Particle Physics and Field Theory, Fudan University, Shanghai 200438, China

Some atomic nuclei exhibit “pear” shapes arising from octupole deformation ( $\beta_3$ ), though direct experimental evidences for such exotic shapes remains scarce. Low-energy model studies suggest  $^{238}\text{U}$  may have a modest octupole deformation arising from collective vibrational degrees of freedom, in addition to a large prolate shape. We investigated the impact of this modest octupole shape on observables involving triangular flow ( $v_3$ ) in high-energy nuclear collisions. Using a hydrodynamic framework, we show  $v_3$  and its correlation with mean transverse momentum,  $\langle v_3^2 \delta p_T \rangle$ , exhibit strong sensitivity to  $\beta_3$ . We found that  $\langle v_3^2 \rangle$  follows a linear increase with  $\beta_3^2$ , while the characteristic anticorrelation in  $\langle v_3^2 \delta p_T \rangle$  shows a pronounced  $\beta_3$ -dependent suppression. Our findings demonstrate that the collective-flow-assisted nuclear imaging method in high-energy nuclear collisions, when compared with experimental data, can provide unique quantitative constraints on higher-order deformations.

*Introduction.*— The atomic nucleus, as a strongly interacting many-body system, exhibits a variety of shapes from spherical to super-deformed [1, 2]. Experimental evidence for nuclear deformation is traditionally extracted from low-energy spectroscopic measurements and models of reduced transition probability between low-lying rotational states, less than a few tens of MeVs/nucleon beam energies [3]. Recent studies have demonstrated that nuclear deformation can be probed in high-energy nuclear collisions in yoctosecond-scale ( $10^{-24}\text{s}$ ) resolution of nuclear many-body distributions by taking advantage of the strong responses of the hydrodynamics collective flow to the shape and size of the initial state [4, 5]. This paradigm has been validated through several experimental measurements at the Relativistic Heavy Ion Collider (RHIC) [6, 7] and at the Large Hadron Collider (LHC) [8, 9], aided by significant theoretical efforts [10–22].

Using this flow-assisted nuclear imaging method, STAR experiment has extracted the shape parameters of the ground-state  $^{238}\text{U}$  nucleus, which has an elongated, axial-symmetric shape with a significant quadrupole deformation ( $\beta_2$ ) and a slight deviation from axial symmetry in the nuclear ground state triaxiality ( $\gamma$ ) [7], consistent with those extracted from low-energy methods. Model studies also reveal the signature of hexadecapole deformation  $\beta_4$  in  $^{238}\text{U}+^{238}\text{U}$  collisions [17, 23, 24]. On the other hand, low-energy experiments and theoretical calculations suggest that  $^{238}\text{U}$  may also exhibit modest octupole collectivity ( $\beta_3$ ) [25–33], but with large uncertainties. This octupole collectivity was traditionally thought to be associated with nuclear vibrational degrees of freedom, rather than static octupole deformation [2, 28, 31, 34]. While  $\beta_4$  naturally couples to  $\beta_2$

and receives a contribution that scales as  $\beta_4 \sim \beta_2^2$ ,  $\beta_3$  represents an independent degrees of freedom orthogonal to even-order deformations. Understanding the nature of octupole deformation of  $^{238}\text{U}$  is crucial for nuclear structure models [35], fission dynamics [36], and may have important implications for fundamental physics – particularly in searches for novel phenomena like atomic electric dipole moments [28, 31, 34, 37, 38]. Here, high-energy nuclear collisions provide, for the first time, a complementary approach to quantify the octupole deformation of  $^{238}\text{U}$  nuclei across energy scales.

*Octupole deformation-triangular flow correlation.*— The sensitivity of heavy-ion collisions to nuclear deformation stems from the approximately linear response relation between the initial-state geometry of the quark-gluon plasma (QGP) and the final-state anisotropic flow. When deformed nuclei collide in random orientations, they imprint distinct spatial anisotropies on the initial energy density profile, characterized by the eccentricity coefficients  $\varepsilon_{n>1} \equiv \left| \int r^n e^{in\phi} e(r, \phi) d^2r / \int r^n e(r, \phi) d^2r \right|$ , where  $e(r, \phi)$  is estimated from the overlap energy density. Driven by pressure gradients, the QGP undergoes hydrodynamic collective expansion, transferring the  $\varepsilon_n$  into azimuthal anisotropy of final-state hadrons. This anisotropy is described by a Fourier expansion of the particle distribution  $dN/d\phi \propto 1 + 2 \sum v_n \cos n(\phi - \Psi_n)$  [39–42]. The elliptic flow  $v_2$  and the triangular flow  $v_3$  capture the hydrodynamic response of the QGP to  $\varepsilon_n$  [43], following a linear relation  $v_n \propto \varepsilon_n$ . Through this relation,  $v_2$  and  $v_3$  become sensitive to quadrupole deformation  $\beta_2$  and octupole deformation  $\beta_3$ , respectively.

Moreover, the event-wise average transverse momentum ( $\langle p_T \rangle$ ) capture the compactness of the QGP, indicated by the inverse area of the overlap  $d_\perp \propto$

$1/\sqrt{\langle x^2 \rangle \langle y^2 \rangle}$  [44], influences the radial expansion or the radial flow, also following a linear relation,  $\delta p_T \propto \delta d_\perp$ , where  $\delta p_T = \langle p_T \rangle - \langle \langle p_T \rangle \rangle$  and  $\delta d_\perp = d_\perp - \langle d_\perp \rangle$  denote event-wise deviations from mean values [7, 45].

In collisions of spherical nuclei,  $\varepsilon_2$  and  $\varepsilon_3$  have different origins: while  $\varepsilon_2$  primarily reflects the impact-parameter-driven overlap ellipticity, non-zero  $\varepsilon_3$  arises solely from random fluctuations of nucleons [46–48]. This leads to an anti-correlation between mass number ( $A$ ) and  $v_3$  in the absence of octupole deformation ( $\beta_3 = 0$ ), where  $\langle v_3^2 \rangle \sim 1/A$ . The presence of  $\beta_3$  and  $\beta_4$  enhances the variance of  $v_n$ , which was found to follow a quadratic form [49] for  $n = 2$  and 3,

$$\begin{aligned} \langle v_2^2 \rangle &\approx a_2 + b_{2,2}\beta_2^2 + b_{2,3}\beta_3^2 + b_{2,4}\beta_2\beta_4, \\ \langle v_3^2 \rangle &\approx a_3 + b_{3,3}\beta_3^2 + b_{3,4}\beta_4^2. \end{aligned} \quad (1)$$

$\beta_4$  can affect  $v_2$  by its non-linear coupling with  $\beta_2$  [17], while  $v_3$  is not expected to be affected by  $\beta_2$  [49]. Here,  $a_n$  encodes the system size and centrality dependence for spherical nuclei, while the coefficients  $b_{n,m}$  are expected to be  $A$  independent. These relations enable a data-driven method to extract the  $\beta_n$  by comparing collisions of two species of similar sizes; see Refs. [10, 49] for details.

In this work, we establish unique experimental signatures for octupole deformation in  $^{238}\text{U}$  using state-of-the-art hydrodynamic modeling. We present quantitative predictions of the impact of  $\beta_3$  using two novel observables,  $\langle v_3^2 \rangle$  and its correlation with transverse momentum  $\langle v_3^2 \delta p_T \rangle$ , in  $^{238}\text{U}+^{238}\text{U}$  collisions, which provide direct benchmarks for forthcoming experimental measurements.

*Hydrodynamic model and observables.*— To identify experimental signatures of octupole deformation in  $^{238}\text{U}$ , we employ the state-of-the-art IP-Glasma+MUSIC+UrQMD model, simulating (2+1)D boost-invariant  $^{238}\text{U}+^{238}\text{U}$  collisions at  $\sqrt{s_{\text{NN}}} = 193$  GeV and  $^{197}\text{Au}+^{197}\text{Au}$  collisions at  $\sqrt{s_{\text{NN}}} = 200$  GeV, respectively. This model consists of an event-by-event initial state model, IP-Glasma [50, 51], coupled with the hybrid framework of relativistic viscous hydrodynamics, MUSIC [52–54], followed by hadronic transport, UrQMD [55, 56]. This model has been tuned to successfully describe collective flow in both small and large systems at RHIC and the LHC [57].

The nucleon density distribution in colliding nuclei is assumed to have a deformed Woods-Saxon form,

$$\begin{aligned} \rho(r, \theta) &\propto (1 + \exp[(r - R(\theta, \phi))/a])^{-1}, \\ R(\theta, \phi) &= R_0(1 + \beta_2[\cos \gamma Y_{2,0} + \sin \gamma Y_{2,2}] \\ &\quad + \beta_3 Y_{3,0} + \beta_4 Y_{4,0}), \end{aligned} \quad (2)$$

where  $R_0 \approx 1.2A^{1/3}$  denotes the nuclear radius,  $a$  is the surface or skin depth, and  $Y_{l,m}(\theta, \phi)$  are the spherical harmonics in the intrinsic frame. The triaxiality parameter

TABLE I. Woods-Saxon parameters used in the simulations of  $^{238}\text{U}+^{238}\text{U}$  and  $^{197}\text{Au}+^{197}\text{Au}$  collisions with IP-Glasma+MUSIC+UrQMD model, where  $d_{\text{min}}$  represents the nucleon minimum distance.

Species	R(fm)	a (fm)	$d_{\text{min}}$ (fm)	$\beta_2$	$\beta_3$	$\beta_4$	$\gamma$ ( $^\circ$ )
$^{197}\text{Au}$	6.62	0.52	0.9	0.14	0	0	45
$^{238}\text{U}$	6.81	0.55	0.9	0.28	0.00, 0.05 0.10, 0.15 0.20	0.09, 0	0

$\gamma$  ( $0^\circ \leq \gamma \leq 60^\circ$ ) governs the relative order of the three principal radii. The nuclear surface  $R(\theta, \phi)$  includes only the most relevant axial symmetric quadrupole, octupole, and hexadecapole deformations [58].

For  $^{197}\text{Au}$ , we adopt  $\beta_{2,\text{Au}} = 0.14$  and triaxiality  $\gamma_{\text{Au}} = 45^\circ$ , inspired by low-energy nuclear structure models that favor a modest oblate deformation [59, 60]. To isolate octupole deformation effects in  $^{238}\text{U}$ , we vary  $\beta_{3,\text{U}}$  from 0 to 0.2 while fixing  $\beta_{2,\text{U}} = 0.28$  and  $\gamma_{\text{U}} = 0^\circ$  (see Tab. I). The effects of hexadecapole deformation are systematically tested by scanning  $\beta_{4,\text{U}}$  between 0 and 0.09 [3, 61, 62]. The minimum nucleon distance in nuclei  $d_{\text{min}}$  is 0.9 fm in these two collision systems. For each parameter configuration, 100k–400k high-statistics hydrodynamic events are generated, allowing the precise determination of shape differences between these two species. Each event is oversampled at least 100 times during the UrQMD stage to ensure enough resolution for anisotropic flow vectors and minimize statistical fluctuations in the hadronic transport.

We analyze a two-particle triangular flow ( $\langle \langle v_3^2 \rangle \rangle$ ) and its correlation with transverse momentum ( $\langle \langle v_3^2 \delta p_T \rangle \rangle$ ) calculated by multi-particle correlations.

$$\begin{aligned} \langle v_3^2 \rangle &= \langle \cos[3(\phi_i - \phi_j)] \rangle_{i,j}, \\ \langle v_3^2 \delta p_T \rangle &= \langle \cos[3(\phi_i - \phi_j)](p_{T,k} - \langle \langle p_T \rangle \rangle) \rangle_{i,j,k}. \end{aligned} \quad (3)$$

Where  $\phi_i$  and  $p_{T,i}$  denote the azimuthal angle and transverse momentum of  $i^{\text{th}}$  particle. The particle indices  $i$ ,  $j$ , and  $k$  are chosen such that only unique combinations are used. The averages are performed first on all multiplets within a single event and then on all events in a fixed centrality bin.  $\langle \langle p_T \rangle \rangle$  represents the event averaged transverse momentum in the ensemble. The value of  $\langle v_3^2 \rangle$  is obtained using the two-subevent method with pseudorapidity gap  $|\Delta\eta| > 1$  and the covariance  $\langle v_3^2 \delta p_T \rangle$  is calculated via the standard method. We verify our results with four different  $p_T$  intervals.

The observables in Eq. (3) are calculated in  $^{238}\text{U}+^{238}\text{U}$  and  $^{197}\text{Au}+^{197}\text{Au}$  collisions, from which we construct the

ratios,

$$R_{v_3^2} = \frac{\langle v_3^2 \rangle_{U+U}}{\langle v_3^2 \rangle_{Au+Au}} \approx \frac{a_{3U}}{a_{3Au}} + \frac{b_{3,3}}{a_{3Au}} \beta_3^2 + \frac{b_{3,4}}{a_{3Au}} \beta_4^2, \quad (4)$$

$$R_{v_3^2 \delta p_T} = \frac{\langle v_3^2 \delta p_T \rangle_{U+U}}{\langle v_3^2 \delta p_T \rangle_{Au+Au}} \approx a - b \beta_2 \beta_3^2. \quad (5)$$

These ratios cancel most of the final state effects and isolate the impact of the deformations. The right-hand sides of these equations, linked to two- and three-body nucleon distributions in the intrinsic frame from Eq. (2), have a simple parametric dependence on shape parameters [49, 63]. The  $a$  and  $b$  terms in Eq. (5) are empirical positive coefficients that change with centrality, proposed in Ref. [63]. Clearly, the sensitivity of  $R_{v_3^2 \delta p_T}$  to octupole deformation requires the presence of large quadrupole deformation, which is nicely fulfilled by  $^{238}\text{U}$  nucleus. This makes  $^{238}\text{U}$  collisions the ideal system for probing  $\beta_3$  effects in heavy nuclei. This particular sensitivity would not be present in  $^{96}\text{Zr}+^{96}\text{Zr}$  vs  $^{96}\text{Ru}+^{96}\text{Ru}$  comparison to constrain the  $\beta_{3,\text{Zr}}$ , given the small values of  $\beta_{2,\text{Zr}}$ .

In Eqs. (4) and (5), we also assume that  $^{197}\text{Au}$  has no higher-order deformations. Otherwise, the constraints derived should be treated as the difference between  $^{238}\text{U}$  and  $^{197}\text{Au}$ , i.e. we need to replace  $\beta_3^2$  by  $\beta_{3,U}^2 - \beta_{3,Au}^2$  etc.

In the absence of deformation, the smaller  $^{197}\text{Au}+^{197}\text{Au}$  collision systems are expected to exhibit stronger fluctuations compared with the larger  $^{238}\text{U}+^{238}\text{U}$  collisions. In this case, we have  $R_{v_3^2} \approx a_{3,U}/a_{3,Au} < 1$ , as well as  $R_{v_3^2 \delta p_T} \approx a < 1$ . The presence of  $\beta_3$  then is to increase the values of  $R_{v_3^2}$  in central collisions to exceed unity. Observation of such a reversal of hierarchy would be a unique signature for  $\beta_3$ . The presence of  $\beta_3$  is expected to reduce the values of  $R_{v_3^2 \delta p_T}$  to further below unity, with the observable transitioning to anti-correlation behavior at large  $\beta_3$  magnitudes. Meanwhile, the presence of  $\beta_4$  is expected to increase  $R_{v_3^2}$  in non-central collisions [49], but its role in  $R_{v_3^2 \delta p_T}$  is unclear. Our findings are discussed with these predictions in mind.

*Results and discussions.*— Figure 1 shows the sensitivity of  $R_{v_3^2}$  on  $\beta_3$  and  $\beta_4$ . Three distinct features are identified: 1) For  $\beta_{3,U} \gtrsim 0.05$ , the ordering of  $\langle v_3^2 \rangle$  in ultra-central collisions (0–2% centrality) is reversed between  $^{238}\text{U}+^{238}\text{U}$  and  $^{197}\text{Au}+^{197}\text{Au}$  collisions, i.e.  $R_{v_3^2} > 1$ . 2) Even outside the ultra-central region, over the 5–20% centrality range,  $\langle v_3^2 \rangle$  is still strongly enhanced by  $\beta_3$ . 3) The  $\beta_4$  increases the values of  $\langle v_3^2 \rangle$  in 5–15% centrality, but has no impact in the ultra-central 0–2% centrality range, consistent with findings from the initial Glauber model [49]. It should be noted that a similar behavior has also been observed in a multi-phase transport model calculations as cross-checks [64]. These trends follow the expectation of Eq. (4) remarkably well, making them robust features that can be verified experimentally. We

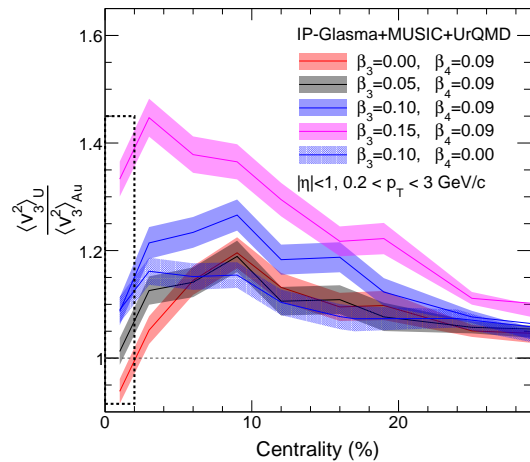


FIG. 1. Ratios of  $\langle v_3^2 \rangle$  between  $^{238}\text{U}+^{238}\text{U}$  and  $^{197}\text{Au}+^{197}\text{Au}$  collisions as a function of centrality for different  $\beta_3$  values from the IP-Glasma+MUSIC+UrQMD calculations. The shaded bands denote the statistical uncertainties. The dashed box marked the 0–2% centrality range that is most sensitive to  $\beta_3$ .

then consider that such a hierarchical feature in 0–2% centrality can be used to set a reliable limit on  $\beta_3$ .

The result of Fig. 1 demonstrates that octupole deformation in  $^{238}\text{U}$  enhances initial-state triangularity ( $\varepsilon_3$ ) beyond the fluctuation-driven baseline for the spherical  $^{197}\text{Au}$  nuclei. As shown in Fig. 1, the statistical uncertainties of current simulations, represented by the shaded bands, are sufficiently small to be sensitive to a modest  $\beta_{3,U}$  value, when compared to the experimental measurements.

Next, we focus on the ultra-central 0–2% centrality

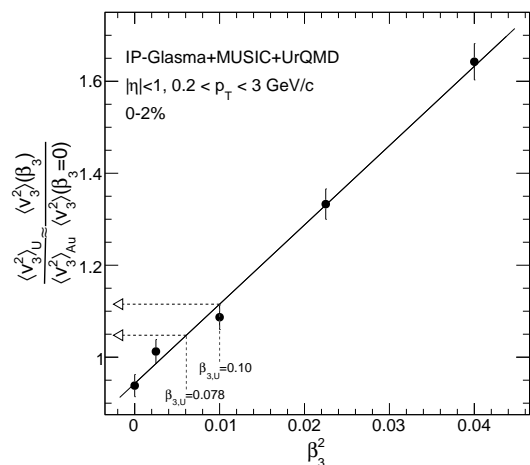


FIG. 2. Predicted  $\langle v_{3,U}^2 \rangle / \langle v_{3,Au}^2 \rangle$  as a function of  $\beta_{3,U}^2$  assuming  $\beta_{3,Au}^2 = 0$  from the IP-Glasma+MUSIC+UrQMD model for 0–2% centrality. The arrows indicate the corresponding values corresponding to  $\beta_{3,U}^2 = 0.078$  and 0.10 from Refs. [26, 29].

range, where the  $R_{v_3^2}$  is mainly sensitive to  $\beta_3$ . Figure 2 shows the predicted ratios as a function of  $\beta_{3,U}^2$ . The ratio follows a linear dependence on  $\beta_3^2$ . Assuming  $\beta_{3,U} = 0.078 - 0.10$  [26, 29, 30], deduced from the nuclear structure predictions, we predict  $R_{v_3^2} \approx 1.05 - 1.12$  indicated by the arrows. This predicted range of the ratio can be readily checked in the future STAR measurement. Experimental results falling within this range could provide direct evidence for octupole deformation in  $^{238}\text{U}$  in high-energy method. We would expect additional sensitivity analyses could provide significant constraints on  $\beta_3$  if the experimental measurements of the ratios achieve sub-percent-level precision.

To gain further insight into nuclear shape, we study the impact of deformation on the three-particle correlator  $\langle v_3^2 \delta p_T \rangle$ . The shape and size of the overlap region from head-on collisions of octupole-deformed nuclei, reflecting the initially produced QGP, directly mirror those of the colliding nuclei projected on the transverse ( $xy$ ) plane. Body-body collisions create a larger, triangular QGP shape with small  $d_\perp$  and large  $\varepsilon_3$ , while tip-tip collisions form a compact, circular QGP exhibiting large  $d_\perp$  and minimal  $\varepsilon_3$ . Certainly, these two configurations exhibit different pressure-gradient-driven expansion patterns, resulting in a pronounced anti-correlation between  $d_\perp$  and  $\varepsilon_3$ . Figure 3 shows  $R_{v_3^2 \delta p_T}$  as a function of centrality for different values of  $\beta_{3,U}$ . In ultra-central collisions,  $R_{v_3^2 \delta p_T}$  exhibits a near-linear dependence on  $\beta_{2,U} \beta_{3,U}^2$ , aligning with the parametric form predicted by Eq. (5), providing complementary insights on the  $\beta_{3,U}$  constrains. The observed enhanced suppression is quantitatively consistent with negative values of  $\langle v_3^2 \delta p_T \rangle$  predicted for strong ‘‘pear’’ shape deformation ( $\beta_{3,U} > 0.15$ ), providing direct evidence for  $^{238}\text{U}$ ’s octupole deformation.

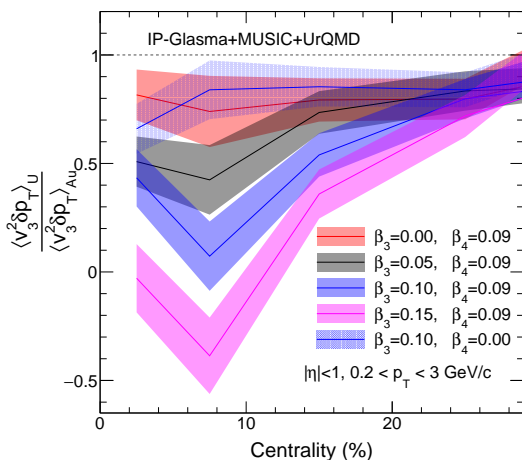


FIG. 3. Ratios of  $\langle v_3^2 \delta p_T \rangle$  between  $^{238}\text{U}+^{238}\text{U}$  and  $^{197}\text{Au}+^{197}\text{Au}$  collisions as a function of centrality for different values of  $\beta_{3,U}$  from the IP-Glasma+MUSIC+UrQMD hydrodynamic model calculations. The shaded bands denote the statistical uncertainties.

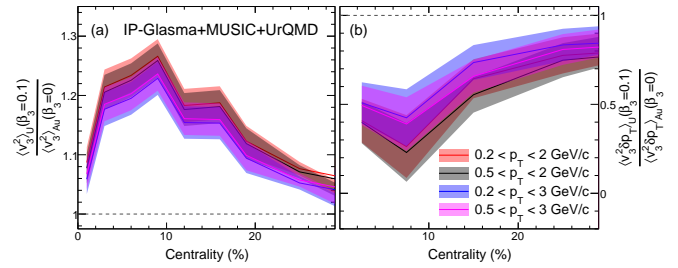


FIG. 4. Centrality dependence of ratios of  $\langle v_3^2 \rangle$  (panel a) and  $\langle v_3^2 \delta p_T \rangle$  (panel b) between  $^{238}\text{U}+^{238}\text{U}$  and  $^{197}\text{Au}+^{197}\text{Au}$  collisions from the IP-Glasma+MUSIC+UrQMD model for four  $p_T$  intervals. The shaded bands denote the statistical uncertainties.

Remarkably,  $R_{v_3^2 \delta p_T}$  also exhibits a sensitivity to  $\beta_{4,U}$ . We observe that  $\beta_{4,U} = 0.09$  alone has a negative contribution that is comparable to  $\beta_{3,U} = 0.10$  alone. However, when both  $\beta_{4,U}$  and  $\beta_{3,U}$  are present, their combined impact is larger. This suggests that terms like  $-\beta_2 \beta_3 \beta_4$  and  $-\beta_2 \beta_4^2$  should be added to Eq. (5) in non-central collisions. For the first time, these couplings imply that the signature of  $\beta_{3,U}$  and  $\beta_{4,U}$  require larger  $\beta_{2,U}$ , making  $^{238}\text{U}$  the ideal nucleus for their observation. Furthermore, the moderate values of  $\beta_{3,U}$  and  $\beta_{4,U}$  ( $\beta_{3,U} \lesssim 0.1$ ,  $\beta_{4,U} \approx 0.05 - 0.1$ ), leads to a  $R_{v_3^2 \delta p_T}$  value within the range of 0.5–1 in the UCC region. Our studies suggest that one should use multiple observables, including  $R_{v_3^2}$  and  $R_{v_3^2 \delta p_T}$ , to simultaneously disentangle the contributions of  $\beta_3$  and  $\beta_4$ .

Another observable often used to study deformation is the normalized quantity  $\rho_3 = \frac{\langle v_3^2 \delta p_T \rangle}{\langle v_3^2 \rangle \sqrt{\langle (\delta p_T)^2 \rangle}}$ . However, the ratio of this quantity  $R_{\rho_3} = \rho_{3,U} / \rho_{3,Au}$  is likely dominated by the deformation impact on  $\langle v_3^2 \rangle$ , and hence is not ideal for our purpose.

Figure 4 shows the centrality dependence of  $R_{v_3^2}$  (panel a) and  $R_{v_3^2 \delta p_T}$  (panel b) calculated in four  $p_T$  intervals with fixed  $\beta_{3,U} = 0.10$ . No variations with the choice of  $p_T$  interval are observed. This implies that the final-state effects are almost completely canceled, leaving the model uncertainties mainly due to the initial conditions. The 20% difference in the mass numbers between  $^{197}\text{Au}$  and  $^{238}\text{U}$  does not lead to any appreciable difference in the hydrodynamic response. The stability of the ratio against varying  $p_T$  intervals is crucial to demonstrate that the impact of nuclear deformation can be measured without the need to impose stringent  $p_T$  selections.

*Summary.*— We employ the state-of-the-art IP-Glasma+MUSIC+UrQMD framework to investigate the effect of high-order deformation on final-state observables in relativistic heavy-ion collisions. The impact of octupole deformation  $\beta_{3,U}$  is revealed by constructing ratios of the same observable between  $^{238}\text{U}+^{238}\text{U}$  and  $^{197}\text{Au}+^{197}\text{Au}$  collisions. The presence of a modest  $\beta_{3,U} \sim 0.1$  should lead to a characteristic reverse ordering

of the  $\langle v_3^2 \rangle$  ratio in 0–2% ultra-central collisions (UCC). On the other hand, the presence of hexadecapole deformation,  $\beta_{4,U}$ , was found to have an impact outside the UCC region. These quantitative predictions can be directly verified by the upcoming measurement from the STAR Collaboration in high-energy nuclear collisions. The ratio of  $\langle v_3^2 \delta p_T \rangle$  was also studied and found to be sensitive to both  $\beta_{3,U}$  and  $\beta_{4,U}$  in a centrality dependent matter. We found that  $\langle v_3^2 \rangle$  follows a linear increase with  $\beta_3^2$ , while  $\langle v_3^2 \delta p_T \rangle$  is suppressed in the presence of  $\beta_3$  in a previously unexplored way. Hence, combining these two ratios can help constrain the upper limit of  $\beta_{4,U}$ , once  $\beta_{3,U}$  is determined. These ratios have also been shown to be insensitive to transverse momentum cuts, indicating the robustness of the determinations of nuclear deformation against kinematic cuts.

Our collective-flow-assisted nuclear imaging approach provides promising path to help reduce the current uncertainties about the QGP initial conditions, particularly its dynamics and transport properties [4, 65, 66]. In addition, this work establishes a potential new avenue for understanding the nature of octupole deformation in heavy nucleus for the first time, which is of major interdisciplinary importance and crucial for nuclear structure physics [31, 32]. This finding naturally leads to the fundamental question of whether the  $\beta_{3,U}$  value extracted from heavy-ion collisions reflects a rigid octupole deformation or octupole vibrational mode in  $^{238}\text{U}$ 's ground state is at least not so clear in low-energy experiments. These results support the idea that heavy-ion collisions can be used as a valuable tool for imaging higher-order nuclear shapes and highlight the applications in tackling many forefront questions in nuclear physics across a wide range of energy scales.

*Acknowledgements.* — We thank P.A. Butler, P. Garrett and G. Giacalone for valuable comments. This work is supported in part by the National Key Research and Development Program of China under Contract Nos. 2024YFA1612600, 2022YFA1604900, the National Natural Science Foundation of China (NSFC) under Contract Nos. 12025501, 12147101, 12205051, the Natural Science Foundation of Shanghai under Contract No. 23JC1400200, Shanghai Pujiang Talents Program under Contract No. 24PJA009, China Postdoctoral Science Foundation under Grant No. 2024M750489. J. Jia and C. Shen are supported by the U.S. Department of Energy, Office of Science, Office of Nuclear Physics, under DOE Awards No. DE-SC0024602 and DE-SC0021969, respectively. C. Shen acknowledges a DOE Office of Science Early Career Award.

---

\* chunjianzhang@fudan.edu.cn

† jiangyong.jia@stonybrook.edu

‡ chenjinhui@fudan.edu.cn

§ chunshen@wayne.edu

¶ liulumeng@fudan.edu.cn

- [1] Kris Heyde and John L. Wood, “Shape coexistence in atomic nuclei,” *Rev. Mod. Phys.* **83**, 1467 (2011).
- [2] David Verney, “History of the concept of nuclear shape,” *Eur. Phys. J. A* **61**, 82 (2025).
- [3] P. Möller, A. J. Sierk, T. Ichikawa, and H. Sagawa, “Nuclear ground-state masses and deformations: FRDM(2012),” *Atom. Data Nucl. Data Tabl.* **109-110**, 1–204 (2016), arXiv:1508.06294 [nucl-th].
- [4] Jiangyong Jia *et al.*, “Imaging the initial condition of heavy-ion collisions and nuclear structure across the nuclide chart,” *Nucl. Sci. Tech.* **35**, 220 (2024), arXiv:2209.11042 [nucl-ex].
- [5] Jiangyong Jia, “Imaging nuclei by smashing them at high energies: how are their shapes revealed after destruction?” (2025), arXiv:2501.16071 [nucl-th].
- [6] Mohamed Abdallah *et al.* (STAR), “Search for the chiral magnetic effect with isobar collisions at  $\sqrt{s_{NN}}=200$  GeV by the STAR Collaboration at the BNL Relativistic Heavy Ion Collider,” *Phys. Rev. C* **105**, 014901 (2022), arXiv:2109.00131 [nucl-ex].
- [7] M. I. Abdulhamid *et al.* (STAR), “Imaging shapes of atomic nuclei in high-energy nuclear collisions,” *Nature* **635**, 67–72 (2024), arXiv:2401.06625 [nucl-ex].
- [8] Shreyasi Acharya *et al.* (ALICE), “Characterizing the initial conditions of heavy-ion collisions at the LHC with mean transverse momentum and anisotropic flow correlations,” *Phys. Lett. B* **834**, 137393 (2022), arXiv:2111.06106 [nucl-ex].
- [9] Georges Aad *et al.* (ATLAS), “Correlations between flow and transverse momentum in Xe+Xe and Pb+Pb collisions at the LHC with the ATLAS detector: A probe of the heavy-ion initial state and nuclear deformation,” *Phys. Rev. C* **107**, 054910 (2023), arXiv:2205.00039 [nucl-ex].
- [10] Giuliano Giacalone, Jiangyong Jia, and Chunjian Zhang, “Impact of Nuclear Deformation on Relativistic Heavy-Ion Collisions: Assessing Consistency in Nuclear Physics across Energy Scales,” *Phys. Rev. Lett.* **127**, 242301 (2021), arXiv:2105.01638 [nucl-th].
- [11] Benjamin Bally, Michael Bender, Giuliano Giacalone, and Vittorio Somà, “Evidence of the triaxial structure of  $^{129}\text{Xe}$  at the Large Hadron Collider,” *Phys. Rev. Lett.* **128**, 082301 (2022), arXiv:2108.09578 [nucl-th].
- [12] Jiangyong Jia, Giuliano Giacalone, and Chunjian Zhang, “Separating the Impact of Nuclear Skin and Nuclear Deformation in High-Energy Isobar Collisions,” *Phys. Rev. Lett.* **131**, 022301 (2023), arXiv:2206.10449 [nucl-th].
- [13] Shujun Zhao, Hao-jie Xu, Yu-Xin Liu, and Huichao Song, “Probing the nuclear deformation with three-particle asymmetric cumulant in RHIC isobar runs,” *Phys. Lett. B* **839**, 137838 (2023), arXiv:2204.02387 [nucl-th].
- [14] Yu-Gang Ma and Song Zhang, “Influence of Nuclear Structure in Relativistic Heavy-Ion Collisions,” in *Handbook of Nuclear Physics*, edited by Isao Tanihata, Hiroshi Toki, and Toshitaka Kajino (2022) pp. 1–30, arXiv:2206.08218 [nucl-th].
- [15] Giuliano Giacalone, Govert Nijs, and Wilke van der Schee, “Determination of the Neutron Skin of Pb208 from Ultrarelativistic Nuclear Collisions,” *Phys. Rev. Lett.* **131**, 202302 (2023), arXiv:2305.00015 [nucl-th].

- [16] Giuliano Giacalone, “Many-body correlations for nuclear physics across scales: from nuclei to quark-gluon plasmas to hadron distributions,” *Eur. Phys. J. A* **59**, 297 (2023), arXiv:2305.19843 [nucl-th].
- [17] Wouter Ryssens, Giuliano Giacalone, Björn Schenke, and Chun Shen, “Evidence of Hexadecapole Deformation in Uranium-238 at the Relativistic Heavy Ion Collider,” *Phys. Rev. Lett.* **130**, 212302 (2023), arXiv:2302.13617 [nucl-th].
- [18] Zhiyong Lu, Mingrui Zhao, Xiaomei Li, Jiangyong Jia, and You Zhou, “Probe nuclear structure using the anisotropic flow at the Large Hadron Collider,” *Eur. Phys. J. A* **59**, 279 (2023), arXiv:2309.09663 [nucl-th].
- [19] Nicolas Miró Fortier, Sangyong Jeon, and Charles Gale, “Heavy-ion collisions as probes of nuclear structure,” *Phys. Rev. C* **111**, L011901 (2025), arXiv:2405.17526 [nucl-th].
- [20] Shujun Zhao, Hao-jie Xu, You Zhou, Yu-Xin Liu, and Huichao Song, “Exploring the Nuclear Shape Phase Transition in Ultra-Relativistic  $^{129}\text{Xe}+^{129}\text{Xe}$  Collisions at the LHC,” *Phys. Rev. Lett.* **133**, 192301 (2024), arXiv:2403.07441 [nucl-th].
- [21] Heikki Mäntysaari, Björn Schenke, Chun Shen, and Wenbin Zhao, “Probing nuclear structure of heavy ions at energies available at the CERN Large Hadron Collider,” *Phys. Rev. C* **110**, 054913 (2024), arXiv:2409.19064 [nucl-th].
- [22] Thomas Duguet, Giuliano Giacalone, Sangyong Jeon, and Alexander Tichai, “Revealing the harmonic structure of nuclear two-body correlations in high-energy heavy-ion collisions,” (2025), arXiv:2504.02481 [nucl-th].
- [23] Hao-jie Xu, Jie Zhao, and Fuqiang Wang, “Hexadecapole Deformation of U238 from Relativistic Heavy-Ion Collisions Using a Nonlinear Response Coefficient,” *Phys. Rev. Lett.* **132**, 262301 (2024), arXiv:2402.16550 [nucl-th].
- [24] Zaining Wang, Jinhui Chen, Hao-jie Xu, and Jie Zhao, “Systematic investigation of the nuclear multipole deformations in U+U collisions with a multi-phase transport model,” *Phys. Rev. C* **110**, 034907 (2024), arXiv:2405.09329 [nucl-th].
- [25] R. H. Spear, “Reduced Electric-Octupole Transition Probabilities,  $B(E3:0(1)+ \rightarrow 3(1)-)$ , for Even-Even Nucleides throughout the Periodic Table,” *Atom. Data Nucl. Data Tabl.* **42**, 55–104 (1989).
- [26] S. E. Agbemava, A. V. Afanasjev, and P. Ring, “Octupole deformation in the ground states of even-even nuclei: a global analysis within the covariant density functional theory,” *Phys. Rev. C* **93**, 044304 (2016), arXiv:1603.03414 [nucl-th].
- [27] D. Ward *et al.*, “Rotational bands in 238 U,” *Nucl. Phys. A* **600**, 88–110 (1996).
- [28] I. Ahmad and P. A. Butler, “Octupole shapes in nuclei,” *Ann. Rev. Nucl. Part. Sci.* **43**, 71–116 (1993).
- [29] F.K. McGowan and W.T. Milner, “Coulomb excitation of states in 238U,” *Nuclear Physics A* **571**, 569–587 (1994).
- [30] T KIBÉDI and R. H SPEAR, “REDUCED ELECTRIC-OCTUPOLE TRANSITION PROBABILITIES,  $B(E3:0\ 1\ + \rightarrow 3\ 1\ -)$ —AN UPDATE,” *Atom. Data Nucl. Data Tabl.* **80**, 35–82 (2002).
- [31] P. A. Butler and W. Nazarewicz, “Intrinsic reflection asymmetry in atomic nuclei,” *Rev. Mod. Phys.* **68**, 349–421 (1996).
- [32] P. A. Butler, “Octupole collectivity in nuclei,” *J. Phys. G* **43**, 073002 (2016).
- [33] S. Zhu, M. P. Carpenter, R. V. F. Janssens, S. Frauendorf, I. Ahmad, T. L. Khoo, F. G. Kondev, T. Lauritsen, C. J. Lister, and D. Seweryniak, “Possible double-octupole phonon band in U-238,” *Phys. Rev. C* **81**, 041306 (2010).
- [34] T. E. Chupp, P. Fierlinger, M. J. Ramsey-Musolf, and J. T. Singh, “Electric dipole moments of atoms, molecules, nuclei, and particles,” *Rev. Mod. Phys.* **91**, 015001 (2019).
- [35] Michael Bender, Paul-Henri Heenen, and Paul-Gerhard Reinhard, “Self-consistent mean-field models for nuclear structure,” *Rev. Mod. Phys.* **75**, 121–180 (2003).
- [36] Guillaume Scamps and Cédric Simenel, “Impact of pear-shaped fission fragments on mass-asymmetric fission in actinides,” *Nature* **564**, 382–385 (2018), arXiv:1804.03337 [nucl-th].
- [37] L. P. Gaffney, P. A. Butler, *et al.*, “Studies of pear-shaped nuclei using accelerated radioactive beams,” *Nature* **497**, 199–204 (2013).
- [38] US Department of Energy (USDOE), *A New Era of Discovery: The 2023 Long Range Plan for Nuclear Science*, Tech. Rep. (US Department of Energy (USDOE), Washington, DC (United States). Office of Science, 2023).
- [39] Arthur M. Poskanzer and S. A. Voloshin, “Methods for analyzing anisotropic flow in relativistic nuclear collisions,” *Phys. Rev. C* **58**, 1671–1678 (1998), arXiv:nucl-ex/9805001.
- [40] Nicolas Borghini, Phuong Mai Dinh, and Jean-Yves Ollitrault, “A New method for measuring azimuthal distributions in nucleus-nucleus collisions,” *Phys. Rev. C* **63**, 054906 (2001), arXiv:nucl-th/0007063.
- [41] Ulrich Heinz and Raimond Snellings, “Collective flow and viscosity in relativistic heavy-ion collisions,” *Ann. Rev. Nucl. Part. Sci.* **63**, 123–151 (2013), arXiv:1301.2826 [nucl-th].
- [42] Jinhui Chen *et al.*, “Properties of the QCD matter: review of selected results from the relativistic heavy ion collider beam energy scan (RHIC BES) program,” *Nucl. Sci. Tech.* **35**, 214 (2024), arXiv:2407.02935 [nucl-ex].
- [43] H. Niemi, K. J. Eskola, and R. Paatelainen, “Event-by-event fluctuations in a perturbative QCD + saturation + hydrodynamics model: Determining QCD matter shear viscosity in ultrarelativistic heavy-ion collisions,” *Phys. Rev. C* **93**, 024907 (2016), arXiv:1505.02677 [hep-ph].
- [44] Björn Schenke, Chun Shen, and Derek Teaney, “Transverse momentum fluctuations and their correlation with elliptic flow in nuclear collision,” *Phys. Rev. C* **102**, 034905 (2020), arXiv:2004.00690 [nucl-th].
- [45] Piotr Bozek and Wojciech Broniowski, “Transverse-momentum fluctuations in relativistic heavy-ion collisions from event-by-event viscous hydrodynamics,” *Phys. Rev. C* **85**, 044910 (2012), arXiv:1203.1810 [nucl-th].
- [46] B. Alver and G. Roland, “Collision geometry fluctuations and triangular flow in heavy-ion collisions,” *Phys. Rev. C* **81**, 054905 (2010), [Erratum: *Phys.Rev.C* 82, 039903 (2010)], arXiv:1003.0194 [nucl-th].
- [47] Derek Teaney and Li Yan, “Triangularity and Dipole Asymmetry in Heavy Ion Collisions,” *Phys. Rev. C* **83**, 064904 (2011), arXiv:1010.1876 [nucl-th].
- [48] Piotr Bozek and Wojciech Broniowski, “Collective dynamics in high-energy proton-nucleus collisions,” *Phys. Rev. C* **88**, 014903 (2013), arXiv:1304.3044 [nucl-th].

- [49] Jiayong Jia, “Shape of atomic nuclei in heavy ion collisions,” *Phys. Rev. C* **105**, 014905 (2022), arXiv:2106.08768 [nucl-th].
- [50] Bjoern Schenke, Prithwish Tribedy, and Raju Venugopalan, “Fluctuating Glasma initial conditions and flow in heavy ion collisions,” *Phys. Rev. Lett.* **108**, 252301 (2012), arXiv:1202.6646 [nucl-th].
- [51] Heikki Mäntysaari, Björn Schenke, Chun Shen, and Prithwish Tribedy, “Imprints of fluctuating proton shapes on flow in proton-lead collisions at the LHC,” *Phys. Lett. B* **772**, 681–686 (2017), arXiv:1705.03177 [nucl-th].
- [52] Bjoern Schenke, Sangyong Jeon, and Charles Gale, “(3+1)D hydrodynamic simulation of relativistic heavy-ion collisions,” *Phys. Rev. C* **82**, 014903 (2010), arXiv:1004.1408 [hep-ph].
- [53] Bjorn Schenke, Sangyong Jeon, and Charles Gale, “Elliptic and triangular flow in event-by-event (3+1)D viscous hydrodynamics,” *Phys. Rev. Lett.* **106**, 042301 (2011), arXiv:1009.3244 [hep-ph].
- [54] Jean-François Paquet, Chun Shen, Gabriel S. Denicol, Matthew Luzum, Björn Schenke, Sangyong Jeon, and Charles Gale, “Production of photons in relativistic heavy-ion collisions,” *Phys. Rev. C* **93**, 044906 (2016), arXiv:1509.06738 [hep-ph].
- [55] S. A. Bass *et al.*, “Microscopic models for ultrarelativistic heavy ion collisions,” *Prog. Part. Nucl. Phys.* **41**, 255–369 (1998), arXiv:nucl-th/9803035.
- [56] M. Bleicher *et al.*, “Relativistic hadron hadron collisions in the ultrarelativistic quantum molecular dynamics model,” *J. Phys. G* **25**, 1859–1896 (1999), arXiv:hep-ph/9909407.
- [57] Bjoern Schenke, Chun Shen, and Prithwish Tribedy, “Running the gamut of high energy nuclear collisions,” *Phys. Rev. C* **102**, 044905 (2020), arXiv:2005.14682 [nucl-th].
- [58] Aage Bohr and Ben R Mottelson, “Nuclear Structure, Vols.I&II,” (1998).
- [59] B. Bally, G. Giacalone, and M. Bender, “The shape of gold,” *Eur. Phys. J. A* **59**, 58 (2023), arXiv:2301.02420 [nucl-th].
- [60] C. Y. Wu and D. Cline, “Triaxiality in quadrupole deformed nuclei,” *Phys. Rev. C* **54**, 2356–2360 (1996).
- [61] C. E. Bemis, F. K. McGowan, J. L. C. Ford, W. T. Milner, P. H. Stelson, and R. L. Robinson, “E-2 and E-4 Transition Moments and Equilibrium Deformations in the Actinide Nuclei,” *Phys. Rev. C* **8**, 1466–1480 (1973).
- [62] J. D. Zumbro, E. B. Shera, Y. Tanaka, C. E. Bemis, R. A. Naumann, M. V. Hoehn, W. Reuter, and R. M. Steffen, “E-2 and E-4 Deformations in U-233, U-234, U-235, U-238,” *Phys. Rev. Lett.* **53**, 1888–1892 (1984).
- [63] Hai-Cheng Wang, Song-Jie Li, Lu-Meng Liu, Jun Xu, and Zhong-Zhou Ren, “Deformation probes for light nuclei in their collisions at relativistic energies,” *Phys. Rev. C* **110**, 034909 (2024), arXiv:2409.02452 [nucl-th].
- [64] Chunjian Zhang and Jiayong Jia, “Evidence of Quadrupole and Octupole Deformations in Zr96+Zr96 and Ru96+Ru96 Collisions at Ultrarelativistic Energies,” *Phys. Rev. Lett.* **128**, 022301 (2022), arXiv:2109.01631 [nucl-th].
- [65] D. Everett *et al.* (JETSCAPE Collaboration), “Multisystem bayesian constraints on the transport coefficients of qcd matter,” *Phys. Rev. C* **103**, 054904 (2021).
- [66] Govert Nijs, Wilke van der Schee, Umut Gürsoy, and Raimond Snellings, “Transverse Momentum Differential Global Analysis of Heavy-Ion Collisions,” *Phys. Rev. Lett.* **126**, 202301 (2021), arXiv:2010.15130 [nucl-th].